



# Testing and Analysis for Lifetime Prediction of Crystalline Silicon PV Modules Undergoing Degradation by System Voltage Stress

## Preprint

Peter Hacke, Ryan Smith, Kent Terwilliger,  
Stephen Glick, Dirk Jordan, Steve Johnston,  
Michael Kempe, and Sarah Kurtz

*Presented at the 2012 IEEE Photovoltaic Specialists Conference  
Austin, Texas  
June 3–8, 2012*

NREL is a national laboratory of the U.S. Department of Energy, Office of Energy Efficiency & Renewable Energy, operated by the Alliance for Sustainable Energy, LLC.

**Conference Paper**  
NREL/CP-5200-54109  
July 2012

Contract No. DE-AC36-08GO28308

## NOTICE

The submitted manuscript has been offered by an employee of the Alliance for Sustainable Energy, LLC (Alliance), a contractor of the US Government under Contract No. DE-AC36-08GO28308. Accordingly, the US Government and Alliance retain a nonexclusive royalty-free license to publish or reproduce the published form of this contribution, or allow others to do so, for US Government purposes.

This report was prepared as an account of work sponsored by an agency of the United States government. Neither the United States government nor any agency thereof, nor any of their employees, makes any warranty, express or implied, or assumes any legal liability or responsibility for the accuracy, completeness, or usefulness of any information, apparatus, product, or process disclosed, or represents that its use would not infringe privately owned rights. Reference herein to any specific commercial product, process, or service by trade name, trademark, manufacturer, or otherwise does not necessarily constitute or imply its endorsement, recommendation, or favoring by the United States government or any agency thereof. The views and opinions of authors expressed herein do not necessarily state or reflect those of the United States government or any agency thereof.

Available electronically at <http://www.osti.gov/bridge>

Available for a processing fee to U.S. Department of Energy and its contractors, in paper, from:

U.S. Department of Energy  
Office of Scientific and Technical Information

P.O. Box 62  
Oak Ridge, TN 37831-0062  
phone: 865.576.8401  
fax: 865.576.5728  
email: <mailto:reports@adonis.osti.gov>

Available for sale to the public, in paper, from:

U.S. Department of Commerce  
National Technical Information Service  
5285 Port Royal Road  
Springfield, VA 22161  
phone: 800.553.6847  
fax: 703.605.6900  
email: [orders@ntis.fedworld.gov](mailto:orders@ntis.fedworld.gov)  
online ordering: <http://www.ntis.gov/help/ordermethods.aspx>

Cover Photos: (left to right) PIX 16416, PIX 17423, PIX 16560, PIX 17613, PIX 17436, PIX 17721



Printed on paper containing at least 50% wastepaper, including 10% post consumer waste.

# Testing and Analysis for Lifetime Prediction of Crystalline Silicon PV Modules Undergoing Degradation by System Voltage Stress

Peter Hacke, Ryan Smith, Kent Terwilliger, Stephen Glick, Dirk Jordan, Steve Johnston, Michael Kempe, and Sarah Kurtz

National Renewable Energy Laboratory (NREL), Golden, CO, 80401, United States

**Abstract** — Acceleration factors are calculated for crystalline silicon PV modules under system voltage stress by comparing the module power during degradation outdoors to that in accelerated testing at three temperatures and 85% relative humidity. A lognormal analysis is applied to the accelerated lifetime test data considering failure at 80% of the initial module power. Activation energy of 0.73 eV for the rate of failure is determined, and the probability of module failure at an arbitrary temperature is predicted. To obtain statistical data for multiple modules over the course of degradation *in-situ* of the test chamber, dark *I-V* measurements are obtained and transformed using superposition, which is found well suited for rapid and quantitative evaluation of potential-induced degradation. It is determined that shunt resistance measurements alone do not represent the extent of power degradation. This is explained with a two-diode model analysis that shows an increasing second diode recombination current and ideality factor as the degradation in module power progresses. Failure modes of the modules stressed outdoors are examined and compared to those stressed in accelerated tests.

**Index Terms** — Degradation, Photovoltaic systems, Photovoltaic cells, Reliability, High-voltage techniques, Current-voltage characteristics.

## I. INTRODUCTION

Determination of the acceleration factors (lifetime at use condition/lifetime at accelerated test condition) for the most relevant PV module degradation mechanisms is a necessary step for the prediction of module lifetime in the field [1]. The relationship between the time to failure of modules undergoing potential-induced degradation (PID) in the field and those in accelerated tests is not yet clarified. Challenges faced include potentially long periods of time before failure is observed in the field. Also, obtaining statistical data of module degradation rates in accelerated lifetime testing presents challenges. While some *in-situ I-V* testing of modules is being carried out in light-soaking chambers for the study of metastabilities in thin film modules, analysis for power degradation generally involves intermittently removing the module from chamber and measuring power on a module tester, which is a time-consuming process when numerous samples are involved. In some cases, transients in power performance may occur while a module is waiting for test. It is conceivable that for these reasons, the level of sophistication in degradation rate analyses and service lifetime forecasting in the PV module world has been relatively low. Along with determination of the acceleration factors, comparing fielded

and chamber-tested modules with modern analytical and imaging tools will be helpful to choose stress levels for accelerated tests that lead to failure modes representative of those in the field.

In this work, we determine a method to accurately and semi-continuously evaluate the power loss of commercial multicrystalline silicon modules by PID *in-situ* of the dark environmental test chamber, avoiding the need for frequent removal of the modules for *I-V* testing with a solar simulator. Multiple replicas of a module design are stressed in damp heat, varying the temperature level. The degradation rate is modeled so that time-to-failure can be extrapolated to arbitrary temperatures. Outdoor tests for system voltage durability are performed with the same module design. The degradation rates and degradation modes of the modules tested outdoors are compared to those in accelerated lifetime testing, and acceleration factors are developed.

## II. EXPERIMENT

Environmental chamber testing was carried out on replicas of a conventional mc-Si module at 50°, 60°, and 85°C, all at 85% relative humidity (RH). The module nameplate system voltage bias of -600 V was applied continuously to the cells in the module by connecting the shorted leads to a high-voltage power supply and grounding the module frame. Dark *I-V* curves were obtained with an *I-V* curve tracer capable of resolving five orders of magnitude in current up to 8 A. Curves for each module were obtained periodically *in-situ* of the chamber after manual disconnection of the high voltage and stabilization of the module temperature to standard test conditions temperature of 25°C and between 40% and 50% RH. Modules were also measured *ex-situ* of the chamber for *I-V* testing with a solar simulator to determine the maximum power ( $P_{\max}$ ) under 1000 W/m<sup>2</sup> illumination before the start of the stress test, when the fraction power remaining was estimated to be in the range of 0.9 to 0.95 and again at ~0.8 or end of test to aid in developing a suitable relationship between the *in-situ* electrical characteristics of the module and  $P_{\max}$ .

Dark *I-V* measurements to evaluate the extent of module degradation in the chamber were recorded *in-situ* and analyzed in three ways. Because the degradation mode for PID in *p*-type base silicon cell modules has been associated with shunting of the cells [2-5], we first determine if we can calculate the module power during PID from the shunt resistance ( $R_{\text{sh}}$ ). In

the first analytical method, the slope in the vicinity of  $V=0$  is measured to determine  $dV/dI$  to estimate  $R_{sh}$ , a simple and convenient gross estimation technique often used by production cell sorters. The analysis of Fahrenbruch and Bube [6] is applied to estimate the power loss of the module, whereby the fraction power loss due to  $R_{sh}$  is given by  $V_{oc}/J_{sc}R_{sh}$ .

In the second technique, a two-diode model (1) was applied to fit the forward bias dark  $I-V$  curves of the modules undergoing degradation [7].  $R_{sh}$  and all the other parameters in the model, including pre-exponentials  $J_{01}$  and  $J_{02}$  and ideality factors  $n_1$  and  $n_2$  within the first and second diode terms referred to respectively as the diffusion and recombination current densities, and the area-specific series resistance  $R_s$ , were varied to achieve fitting of the dark  $I-V$  curve. The ideality factors of the first and second diode terms are often given respectively as 1 and 2 in textbooks; however, it has been found that ideality factor further increases in cells with crystallographic defects or a high density of states in the p-n junction [7]. The two-diode model dark  $I-V$  curve fitting has also been described by King and coworkers for analysis of module degradation [8]. As in the first analysis, the evolving  $R_{sh}$  is evaluated for the goal of determining the module power degradation.

$$J = J_L - J_{01} \left\{ \exp \left[ \frac{q(V+JR_s)}{n_1 kT} \right] - 1 \right\} - J_{02} \left\{ \exp \left[ \frac{q(V+JR_s)}{n_2 kT} \right] - 1 \right\} - \frac{V+JR_s}{R_{sh}} \quad (1)$$

The third technique applied was based on superposition—the simplifying assumption that the  $I-V$  curve obtained in the dark can be translated from the first quadrant to the fourth quadrant by subtracting the photocurrent [9]. Photocurrent (at  $J_{sc}$ ) of the module undergoing PID has been observed to be relatively constant [2,4]. The maximum power point is then evaluated on the translated  $I-V$  curve as is conventionally done for curves obtained with solar simulators. This value determined from the dark  $I-V$  data is compared to the periodically measured power obtained with a solar simulator to determine if a relationship can be made. We then determine how the module power estimated from the dark  $I-V$  data obtained in the environmental chamber can be used to predictively extrapolate failure times and failure distributions.

Outdoor degradation experiments were performed on replicas of the module design tested in damp heat chambers in Florida, USA, to obtain representative module performance under the natural stresses of a humid subtropical climate. Negative 600 V bias was applied to the leads of these modules over a load resistor during the day logarithmically with irradiance to simulate the voltage experienced by the cells in a high negative voltage module string. The modules were mounted horizontally to represent a relatively stressful but realistic flat roof mounting configuration. The modules were periodically dismantled to evaluate their  $I-V$  characteristics under a solar simulator. The time-to-failure of modules stressed outdoors are compared to those stressed in the

accelerated tests at several temperatures to determine the acceleration factor as a function of temperature.

Finally, to determine the onset of various failure modes as a function of stress level and to choose stress levels in accelerated testing that are relevant to the degradation modes of fielded modules, a group of one-cell mc-Si mini-modules with a conventional construction — glass, ethylene-vinyl acetate, and polyester/polyvinyl fluoride backsheets — were constructed and exposed to increasing levels of temperature and humidity. Negative 1000 V bias was first applied to the active layer, followed by a recovery with positive 1000 V bias, each for 120 h. Testing in both polarities is necessary as cells may show sensitivity to either polarity depending on the cell design [10]. This sequence was repeated incrementally at higher temperature and RH combinations. Carbon-containing paste was applied over the glass face to induce through-glass current flow. This is expected to have the effect of accelerating PID at the lower temperatures and RH, where the glass surface would normally exhibit less conductivity to ground. The samples were given one week in the chamber at the step level temperature and humidity before voltage was applied. Optical, electroluminescence (EL), and in selected cases, photoluminescence imaging was performed to differentiate series resistance and recombination losses.

### III. RESULTS AND DISCUSSION

#### A. Estimation of power loss from shunt resistance

The shunt resistance of a module, as estimated from the value of  $dV/dI$  in the vicinity of  $V=0$ , was measured in the environmental chamber at 25°C after an exposure to 85% RH, 85°C, and -600 V bias. The power remaining at the end of the test based on the  $R_{sh}$  estimation was  $0.942 \cdot P_{max,0}$ , which correlates very poorly with the actual power drop to  $0.765 P_{max,0}$  determined by a solar simulator (Table 1). It is found that the shunt resistance as captured by the slope in the dark  $I-V$  curve does not capture the dominant factor causing the power loss that is observed in the module, and despite the method's attractive simplicity, it does not appear to be a suitable technique for evaluating module power loss from PID.

TABLE I  
SHUNT RESISTANCE OF A MODULE DEGRADED BY POTENTIAL-INDUCED DEGRADATION ESTIMATED FROM  $dV/dI$  AT  $V \approx 0$  AND BY THE TWO-DIODE MODEL, RESULTING FRACTION POWER LOSS, AND ACTUAL FRACTION POWER LOSS DETERMINED BY A SOLAR SIMULATOR. THE INITIAL SHUNT RESISTANCE OF CELLS WITHIN THIS MODULE WAS  $\sim 6 \text{ k}\Omega \cdot \text{cm}^2$ .

	$dV/dI$ at $V \approx 0$	Two-diode	Solar simulator
$R_{sh} (\Omega \cdot \text{cm}^2)$	333	660	
$P_{max}/P_{max,0}$	0.942	0.971	0.765

The entire dark  $I-V$  curve of the modules undergoing PID in chamber was then analyzed by curve fitting to determine the evolution of  $R_{sh}$  and other lumped diode parameters of the

two-diode model. The analysis indicates the  $J_{02}$  parameter, inclusive of any non-ohmic leakage current through the cells, is increasing by two orders of magnitude over the course of the test, ideality factor  $n_2$  increases, and  $R_{sh}$  decreases gradually to  $660 \Omega\text{-cm}^2$ . The module power associated with the  $R_{sh}$  decrease calculates out to be only  $0.971 \cdot P_{\max_0}$ , compared to  $0.765 \cdot P_{\max_0}$  actual degradation for this module. The increase in the non-linear recombination current of the second diode term of the two-diode model is thus an important component of PID. For this reason, it appears that using  $R_{sh}$  alone will not predict power of the module undergoing PID.

### B. Estimation of power loss from superposition of the dark I-V curve

The principle of superposition using the dark I-V curve was applied for the determination of  $P_{\max}$ . All dark I-V curves were translated to the fourth quadrant by 7.3 A (30 mA/cm<sup>2</sup> for the encapsulated 15.6 cm x 15.6 cm area cells). The maximum power points obtained from the translated 25°C dark I-V curves were compared to those obtained with a solar simulator captured up to three times each for all replicas among two module designs undergoing PID in the environmental chamber, and the correlation was found to be excellent (Fig. 1). The dark I-V curves can therefore be used to estimate the PID *in-situ* of the chamber, whereby numerous data points can be obtained, enabling statistical modeling for goals such as service life prediction. This analysis eliminates the need for frequent removal of the module for testing under a solar simulator.

Chamber temperature was ramped to 25°C for capture of the dark I-V curve that was used for the data presented herein. Measurement of I-V curves at the elevated stress temperatures were also carried out and translation coefficients to relate  $P_{\max}$  obtained at the stress temperature to standard test condition (25°C) could be used. It is anticipated that such analysis will be developed in more depth in a future publication. Superposition may not be as readily applicable to the *in-situ* monitoring of all failure modes in accelerated testing. Despite superposition's success in relating dark I-V curves to  $P_{\max}$  determined by the solar simulator for the effects of system voltage stress in damp heat in conventional Si modules, further tests are required to determine the applicability of this method to other stress factors and degradation mechanisms.

### C. Degradation modeling of the accelerated lifetime test data

The degradation in power of one module design at 85°C (three replicas), 60°C (two replicas), and 50°C (three replicas), 85% RH, and -600 V bias in an environmental chamber was monitored using the estimation of power loss from superposition of the dark I-V curves discussed above. It was found that the power drop could be modeled linearly by transforming the time axis scale to the power of two as shown in Fig. 2. The residuals in the linear fitting are shown in the inset. It can be seen that the reproducibility in degradation rates of the various samples is good, with the exception of a

few outliers in the most highly accelerated test (85°C). More work is necessary to derive a mechanistic function, which is anticipated to further improve the degradation curve fitting. Further, automation of the switching between application of the high voltage bias and sweeping of the dark I-V curve to increase the frequency of the data taking will better resolve the degradation curves. The degradation data was then analyzed with lognormal statistics, and a lifetime prediction plot was created to calculate the probability of module failure at arbitrary temperatures at 85% RH with a  $0.8 \cdot P_{\max_0}$  failure criterion (Fig. 3). As an example, the failure probability distribution is calculated and shown for the case of stress at 25°C, where it is indicated that the peak probability for time-to-failure is around 550 h.

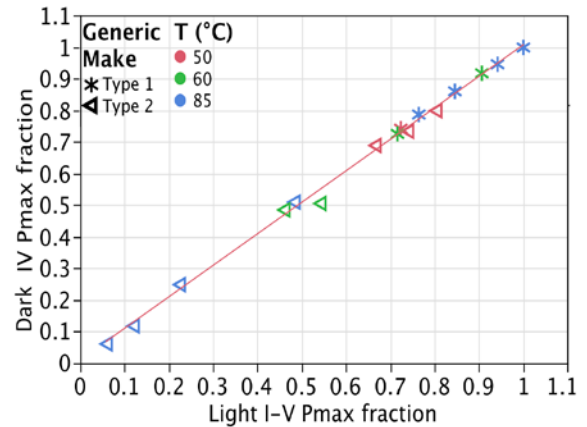


Fig. 1. Correlation between module power ( $P_{\max}$ ) determined from the 25°C dark I-V curves translated to the fourth quadrant (i.e., superposition) and the solar simulator for two module types over the course of PID at -600 V, 85% RH. The correlation is found to be excellent over the whole range of degradation for thirteen modules stressed at various temperatures as shown.

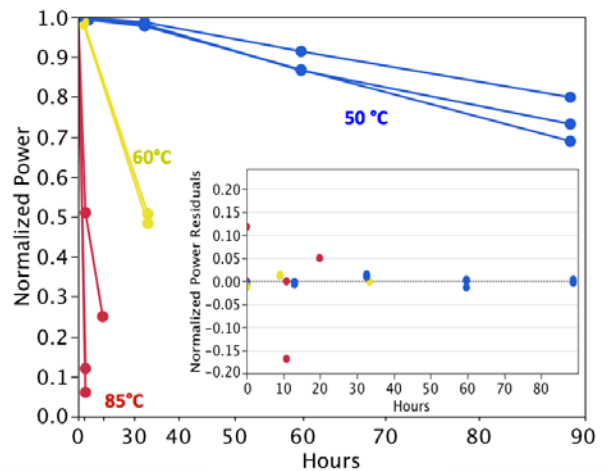


Fig. 2. Normalized power of PV modules undergoing potential induced degradation at 85% RH, -600 V bias, and at three temperatures indicated on the plot. The data is fit linearly with the time (h) scaled to the power of two. Residuals to the fit are shown in the inset.

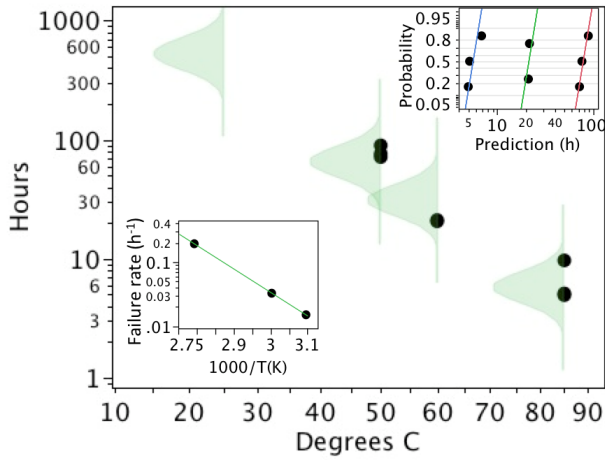


Fig. 3. Lifetime prediction plot as a function of temperature for 85% RH based on failure data interpolated from the degradation curves generated in accelerated lifetime testing. The density curves indicating probability of module failure are shown overlaying the points of failure at the  $0.8 \cdot P_{\max_0}$  level, and the density curve extrapolated to  $25^\circ\text{C}$  is also shown. A multiple probability plot shows a lognormal distribution with the same shape factor to be a good fit to the data (upper right inset). The activation energy for the statistically determined rate of failure is  $0.726 \pm 0.053$  eV (lower left inset).

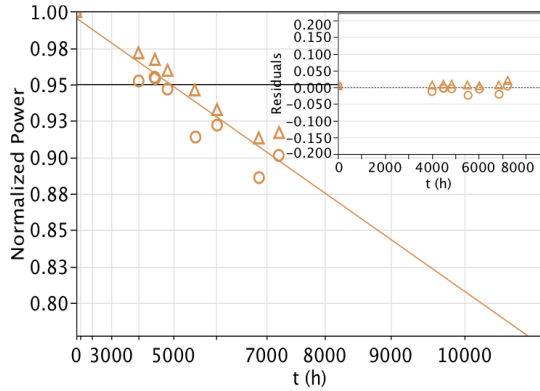


Fig. 4. Fraction power remaining as a function of time under  $-600$  V system voltage bias (applied logarithmically with irradiance) for two module replicas ( $\circ, \Delta$ ) fielded in Florida, USA, for approximately 10 months exhibiting PID. For comparison, these modules are of the same design studied in the accelerated lifetime testing.

#### D. Degradation rates of fielded modules and determination of acceleration factors

The power as a function of time for two replicas of the module design discussed above that was mounted in Florida, USA, under system voltage bias is shown in Fig. 4. As was done for the accelerated lifetime test data, the power loss is successfully fit linearly with the time scale squared. Failure in this case is taken at  $0.95 \cdot P_{\max_0}$ , the degradation limit typical of PV module qualification testing. The alternative,  $0.8 \cdot P_{\max_0}$ , a common module warranty limit, leads to censoring as the modules have only degraded to  $0.89 \cdot P_{\max_0}$  at this writing. The fitting curve in Fig. 4 is nevertheless extrapolated to  $0.8 \cdot P_{\max_0}$ , showing the estimation of warranty failure at about  $12,000$  h ( $1.37$  y).

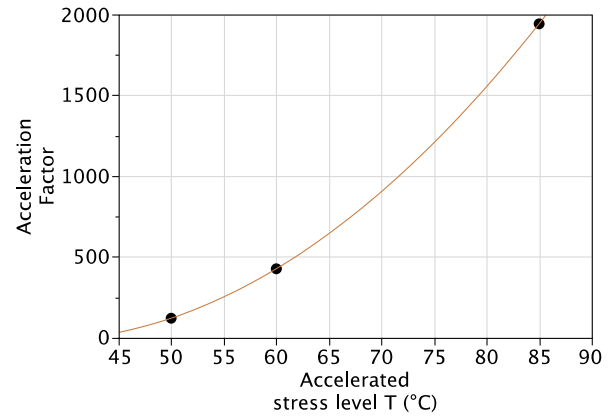


Fig. 5. Acceleration factor for the PV module design mounted in Florida USA, and undergoing accelerated testing at 85% RH, applied module system voltage of  $-600$  V, temperatures as shown, and failure defined at  $0.95 P_{\max_0}$ .

To determine the time to failure of the fielded module from accelerated lifetime testing, the acceleration factor is calculated—the lifetime at use level/lifetime at accelerated stress level. In this case, the use level is the Florida environment, where the degradation as a function of time is shown in Fig. 4 and the accelerated test stress level is 85% RH with temperature levels at  $50^\circ\text{C}$ ,  $60^\circ\text{C}$ , and  $85^\circ\text{C}$  shown in the data of Fig. 2. The system voltage in all cases is  $-600$  V, and the failure is again considered at  $0.95 \cdot P_{\max_0}$ . The calculated acceleration factors determined at each stress level of the accelerated tests are graphed in Fig. 5, and the points are interpolated with a fitting curve.

#### E. Imaging of PID modules for determination of failure modes

In the choice of accelerated test conditions, it is necessary to generate the degradation modes that are seen in the field. The degradation modes with voltage bias applied under acceleration as a function of temperature and RH stepped through increasingly higher levels are shown in Fig. 6. After  $50^\circ\text{C}$ , 50% RH, regions of emerging PID is evident by the new dark regions in the EL and corresponding regions of high current flow through the junction in the thermography (Fig. 6). After  $70^\circ\text{C}$ , 70% RH, there is evidence of the deep-blue silicon nitride coating giving way to brown or the grey color of silicon at the top of the cell. This is believed to be associated with the decomposition of silicon nitride to hydrous silica and ammonia in the presence of high chemical activity of water [11]. After  $85^\circ\text{C}$ , 85% RH, there is also evidence of series resistance increase in some dark areas of the EL image considering the corresponding areas of the thermography indicate cold regions where current does not flow. The series resistance increase is confirmed by photoluminescence imaging of this sample after  $85^\circ\text{C}$ , 85% RH exposure in Fig. 7. The series resistance increase around the upper bus bar ribbon may be associated with the dissolution of the glass-rich interface between the Ag grid-finger contacts and the silicon cell, possibly enabled by residual acid solder flux, acetic acid from the encapsulant, elevated humidity within the package, and electrolytic corrosion from the applied voltage bias.

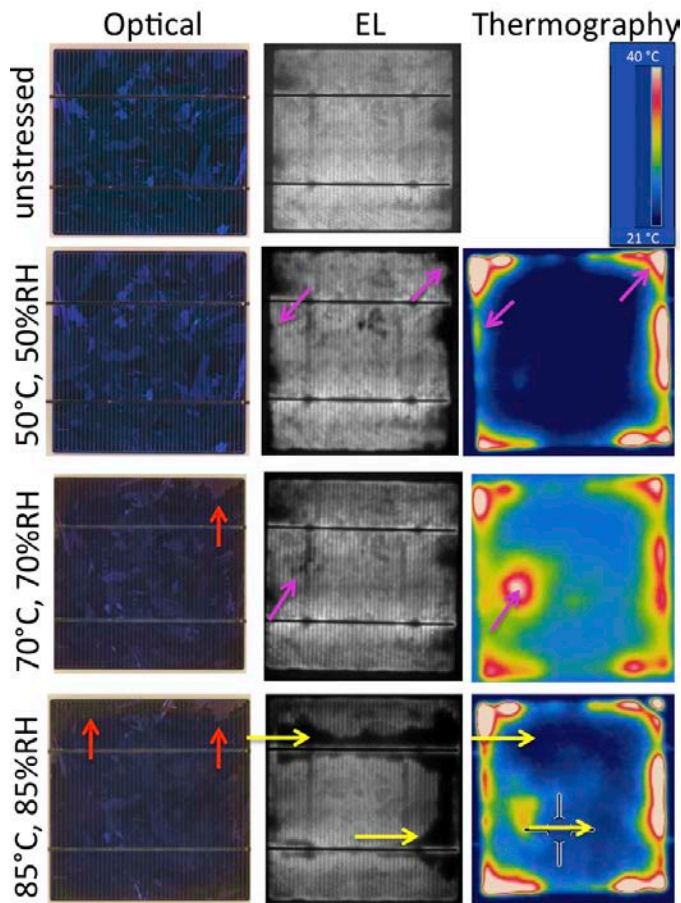


Fig. 6. Imaging—optical, electroluminescence (EL) under forward bias, and reverse bias thermography—of one-cell mini-modules stressed alternately for 120 h periods at negative and positive 1000 V, at increasingly higher levels of environmental stress, as shown after the negative bias cycle. After 50°C, 50% RH exposure, PID by junction leakage is evident by new dark regions in the EL associated with non-radiative recombination and corresponding regions of high current flow through the junction in the thermography indicated by the purple arrows. After 70°C, 70% RH exposure, there is evidence of silicon nitride degradation at the top face of the cell (red arrow) and additional PID by junction leakage (purple arrows). After 85°C, 85% RH exposure, there is additional silicon nitride degradation (red arrows) and new evidence of series resistance increase in the dark areas of the EL and the cool areas of the thermography image (yellow arrows).

Degradation modes of a module stressed outdoors are then examined. Early failures of the most severely stressed modules fielded in Florida under -1500 V bias degraded to 0.35 of the initial power exhibit regions of high current flow through the junction indicated in EL and thermography (Figs. 8a and b). Inspecting by photoluminescence confirms the areas of carrier recombination and further shows no regions of high series resistance (Figs. 8c and d). While further study of outdoor failures over many module designs and locations are required, it appears that the 70°C, 70% RH and greater condition may manifest in additional failure modes such as silicon nitride degradation and cell series resistance increases that are not yet

confirmed to occur in the field. Further exploration of these failure modes in fielded modules is required to find evidence of the modes we seek to accelerate and predict.

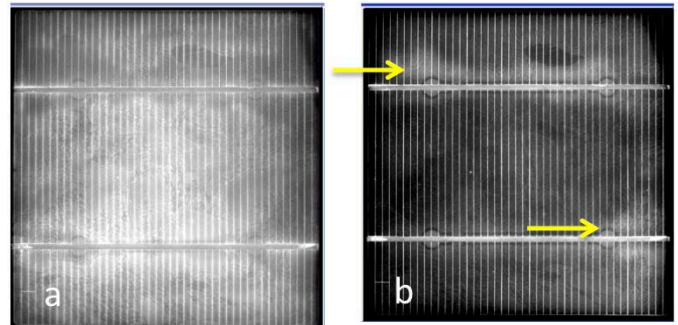


Fig. 7. Photoluminescence of a cell after exposure at 85°C, 85% RH, -1000 V bias. (a) Cell at open-circuit voltage, where darker regions indicate non-radiative recombination; (b) short circuit, where light regions such as those indicated by arrows indicate elevated series resistance. Both junction recombination or shunting losses and series resistance modes are seen to be active after this stress level.

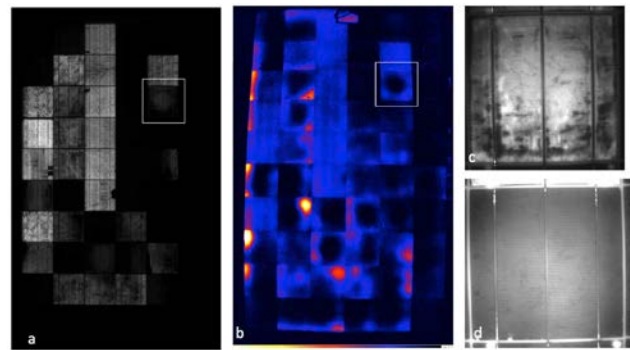


Fig. 8. Module mounted in Florida, USA, after 10 months with the active layer biased at -1500 V scaled with irradiance, degraded to 0.35  $P_{\max_0}$ . (a) EL image; (b) thermography of same module (bright areas are hot); (c) photoluminescence in open circuit of cell indicated by white square (dark areas indicate non-radiative carrier recombination); (d) photoluminescence in short circuit (light areas indicate elevated series resistance). Gradual gradients across the surface are due to non-uniform illumination, thus there is no evidence of elevated series resistance in the fielded modules.

#### IV. SUMMARY AND CONCLUSIONS

Dark  $I-V$  curves measured *in-situ* in an environmental chamber and analyzed by superposition were used to accurately, rapidly, and statistically evaluate module power during PID. The degradation curves were linearized by evaluating the rate on a time squared scale and used to model the anticipated lifetime as a function of temperature in 85% RH. The acceleration factor for PID as a function of temperature was determined for a commercial module design at the rated system voltage (-600 V) in Florida, USA, so that lifetime associated with the PID failure mode may be forecasted by accelerated testing. It was seen that higher stress levels, such as those around and above 70°C, 70% RH, lead to high chemical activity of water that leads to degradation

modes such as silicon nitride degradation and series resistance increases that we have not yet seen in the field.

#### ACKNOWLEDGMENT

The authors thank Allen Anderberg, Steve Rummel, Keith Emery, Fei Yan, Bill Sekulic, Keith Showalter and Stephen Barkaszi for assistance with measurements and helpful discussions and Michael Köhl for review of the manuscript. This work was supported by the U.S. Department of Energy under Contract No. DE-AC36-08-GO28308 with the National Renewable Energy Laboratory.

#### REFERENCES

- [1] T. J. McMahon, "Accelerated Testing and Failure of Thin-film PV Modules," *Prog. Photovolt: Res. Appl.* **12**, 2004, pp. 235–248.
- [2] H. Nagel, et al., "Crystalline Si Solar Cells and Modules Featuring Excellent Stability Against Potential-Induced Degradation," *26th European Photovoltaic Solar Energy Conference and Exhibition*, 2011, Hamburg.
- [3] P. Hacke et al., "Test-to-Failure of Crystalline Silicon Modules," *35th IEEE PVSC*, Honolulu, 2010, pp. 244–250.
- [4] S. Pingel et al., "Potential Induced Degradation of Solar Cells and Panels," *35th IEEE PVSC*, Honolulu, 2010, pp. 2817–2822.
- [5] M. Schütze et al., "Laboratory study of potential induced degradation of silicon photovoltaic modules," *37th IEEE PVSC*, Seattle, 2011, in print.
- [6] A. L. Fahrenbruch and R. H. Bube, *Fundamentals of Solar Cells: Photovoltaic Solar Energy Conversion*, Academic Press, 1983, pp. 220–222.
- [7] O. Breitenstein, et al. "Influence of Defects on Solar Cell Characteristics," *Solid State Phenomena* Vols. 156-158 (2010) pp. 1-10.
- [8] D. L. King, et al., "Dark current-voltage measurements on photovoltaic modules as a diagnostic or manufacturing tool," *26th IEEE PVSC*, 1997, pp. 1125–1128.
- [9] M. Wolf and H. Rauschenbach, "Series resistance effects on solar cell measurements," *Advanced Energy Conversion*, **3**, pp. 455–479, Pergamon, 1963.
- [10] R. Swanson, et al., "The Surface Polarization Effect in High-Efficiency Silicon Solar Cells," *15th PVSEC*, Shanghai, China, 2005.
- [11] K. Morita and K. Ohnaka, "Novel Selective Etching Method for Silicon Nitride Films on Silicon Substrates by Means of Subcritical Water," *Ind. Eng. Chem. Res.*, **39**, 2000, pp. 4684–4688.